DE GRUYTER OPEN

Journal of ELECTRICAL ENGINEERING, VOL 69 (2018), NO1, 24–31

Scanning electron microscope fine tuning using four-bar piezoelectric actuated mechanism

Khaled S. Hatamleh[*,**], **Qais A. Khasawneh**[*,***], **Adnan Al-Ghasem**[*,****]
Mohammad A. Jaradat[*,**], **Laith Sawaqed**[*], **Mohammad Al-Shabi**[*****]

Scanning Electron Microscopes are extensively used for accurate micro/nano images exploring. Several strategies have been proposed to fine tune those microscopes in the past few years. This work presents a new fine tuning strategy of a scanning electron microscope sample table using four bar piezoelectric actuated mechanisms. The introduced paper presents an algorithm to find all possible inverse kinematics solutions of the proposed mechanism. In addition, another algorithm is presented to search for the optimal inverse kinematic solution. Both algorithms are used simultaneously by means of a simulation study to fine tune a scanning electron microscope sample table through a pre-specified circular or linear path of motion. Results of the study shows that, proposed algorithms were able to minimize the power required to drive the piezoelectric actuated mechanism by a ratio of 97.5 % for all simulated paths of motion when compared to general non-optimized solution.

K e y w o r d s: piezoelectric, inverse kinematics optimization, four-bar mechanism, power minimization

1 Introduction

Four bar mechanisms can be used in many applications. One of those applications is the Scanning Electron Microscope (SEM) in which fine tuning is essential to explore micro-scale images. For instance, in order to navigate through nanowires image shown in Fig. 1(a), it is needed to zoom out and move the specimen to another location and then zoom in again, which causes loss of wire location, hence in this paper a four bar mechanism is proposed to be able to track and navigate through small images like a single nanowire image shown in Fig. 1(b) without the need to zoom in and out. The proposed mechanism schematic is shown in Fig. 2.

Many researchers investigated four bar mechanisms and PZT mechanisms for many applications and in different fields, such as; mechanical systems, MEMS and NEMS, bio technology, and much more. Bhagyesh *et al* developed a four bar compliant mechanism using pseudo rigid body model (PRBM) incorporating a micro-slide actuator in an experimental setup, experimental results validated the finite element analysis of the proposed simplified PRBM mechanism [1]. On the other hand, Madhab *et al* presented a mathematical model of PRBM for a four bar based complaint micro-manipulator to control a bio-inspired micro-gripper, through obtaining the relationship between the input force and displacement [2].

In [3], a mathematical model of a piezo actuated positive displacement compressor was formulated. It has been found that the performance was greatly influenced by the stiffness and operational frequency of piezo-actuator. An expanded literature review regarding piezo and pyroelectric microscopy experimental techniques was presented by Athanasios *et al*, the review addressed resolution of

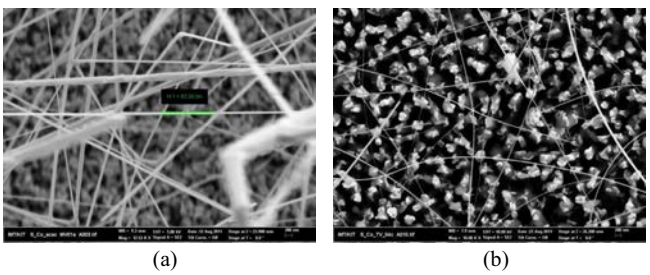

(a) (b)

Fig. 1. (a) – nanowires image, (b) – single nanowire image

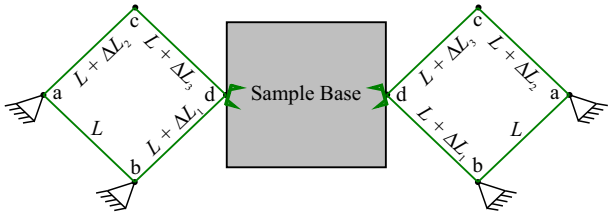

Fig. 2. Proposed four bar peizoelectric actuated mechasim for SEM micro tuning

* Mechanical Engineering Department, Jordan University of Science & Technology, PO Box 3030 Irbid, Jordan, khatamleh@aus.edu, ** Mechanical Engineering Department, American University of Sharjah, PO Box (2666) Sharjah, UAE., *** Electromechanical Engineering Department, Institute of Applied Technology, Abu Dhabi, UAE, **** Mechanical engineering Department, Fahad bin Sultan University, POBox 15700, Tabuk, KSA, ***** Mechanical Engineering Department, University of Sharjah, PO Box (27272) Sharjah, UAE

DOI: 10.1515/jee-2018–0003, Print (till 2015) ISSN 1335-3632, On-line ISSN 1339-309X

(1 μm–10 μm) and stimulus in terms of thermal wave, pressure pulse, and voltage [4].

Recently Boukari presented a computational efficient model for piezoelectric actuators taking into consideration the non-linear effects resulting from hysteresis [5]. Moreover, a new pyramidal shape 3-DOF piezo driven mechanism subjected to different phases and frequencies was proposed, modeled, manufactured and tested. The response of the mechanism tip for both linear and non-linear inputs signals was investigated [6].

Precision machinery requires micro-positioner that can be achieved using piezo actuators. Non-linearties (hysteresis) and tracking errors in piezo actuators is a known issue and can be solved and overcome by using a controller. A proposed adaptive sliding mode controller for a 3D PZT actuated table for drilling process was introduced and analyzed. The study recommended a control solution that addressed hysteresis and tracking errors of PZT actuators [7], while a flexure based mechanism and control methodology for ultra-precision turning table operation was introduced in [8]. Moreover, Qingsong Xu presented the design and model analysis of a novel compact long-stroke precision positioning stage in [9]. The study carried out finite Element analysis and experimental testing of PID and Discrete Time Sliding Control (DTSC) over the presented mechanism to follow a pre-specified path. Results showed that DTSC overcame PID control in terms of accuracy and robustness with the presence of system uncertainties.

A robust motion tracking control for micro/nano manipulators dealing with non-linarites, external disturbances and unknown or uncertain system parameters was proposed in [10]. The controller was based on known estimated lump parameters of the flexure four bar mechanism and its capability of motion tracking. In addition, robust generalized impedance control methodology including force trajectories and enhanced adaptive motion tracking control including angular stiffness of flexure hinged were presented in [11]. Other advanced control strategies were proposed to achieve faster response and more accurate control performance for nano positioning and manipulation applications, such as the integrated control strategy proposed in [12] for PZT nano-positioning stages, and the feed-forward and feedback compound controller of the decoupled XY stage model established in [13].

To enhance the accuracy and the response, and reduce power consumptions; other methods including H^{∞} based loop shaping control scheme [14], least square optimization [15], multi-objective genetic algorithm optimization [16] and heuristic optimization algorithm [17], were combined in synthesis and control of multi bar mechanisms.

2 Modeling of proposed piezoelectric actuated four bar mechanism

Several piezoelectric actuated four bar mechanisms (PZT-FBM) were presented with one or two-piezoelectric actuated links [11, 18–24]. These links were proposed to be utilized in different applications at small or macro/micro scales. For instance a PZT-mechanism was utilized for hard disk drive head fine positioning as shown in Fig. 3 [23]. However, such mechanism has a limited workspace as illustrated by Fig. 4, which does not satisfy the work space required by the SEM fine tuning mentioned earlier. In this study a four-bar mechanism with three-piezoelectric links will be considered. The mechanism has been introduced by the authors in an earlier study to move an inchworm robot [24], the attainable workspace by the SEM using the proposed mechanism is wider than that manageable by two-piezoelectric four bar mechanism introduced in [23].

Figure 5 illustrates a four bar parallel mechanism that consists of one fixed link of length L, and three other piezoelectric actuated links. The initial length of all bars (when no piezoelectric actuation is introduced) is equal to L. If piezoelectric material of link-i is actuated, a change of length δL_i will take place such that $L+\Delta L_i$. Positive polarity of the actuation signal introduces an elongation over δL_i, while negative polarity causes a shorter link length.

Square (abdc) of Fig. 5 represents the initial position of the mechanism with the End Effector EE point represented by point d. Quadrilateral (abef) represents an actuated position of the mechanism with the EE (point

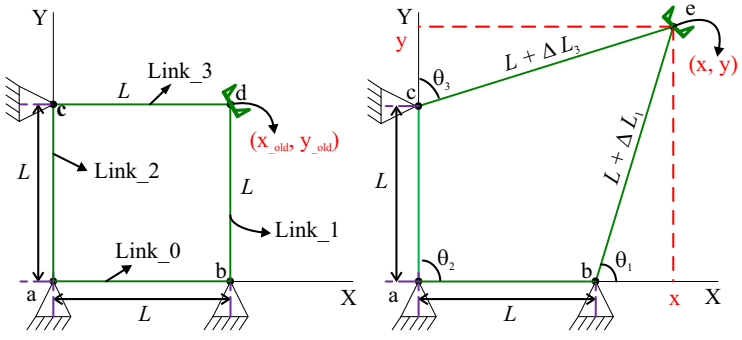

Fig. 3. Four bar mechanism with two-piezoelectric actuated links

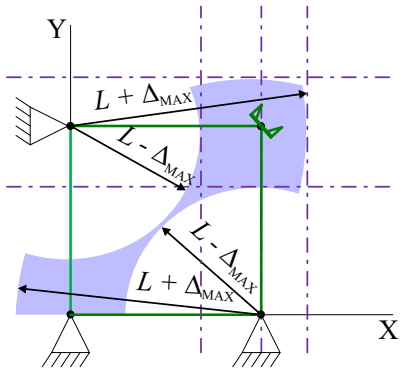

Fig. 4. Work space of four bar mechanism with two-piezoelectric actuated links

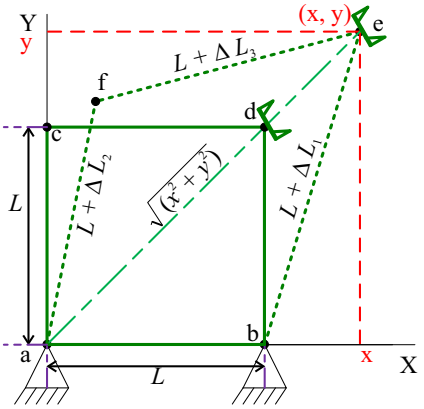

Fig. 5. Four bar mechanism with three-piezoelectric actuated links

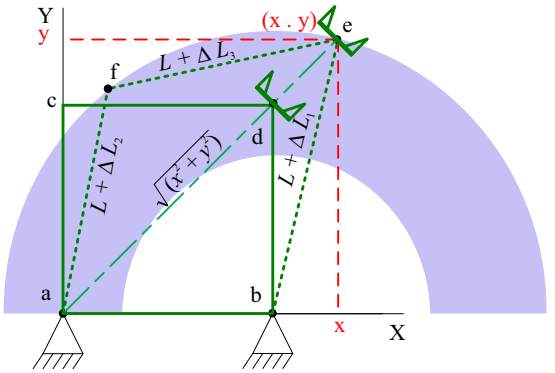

Fig. 6. Four bar mechanism with three-piezoelectric bars workspace

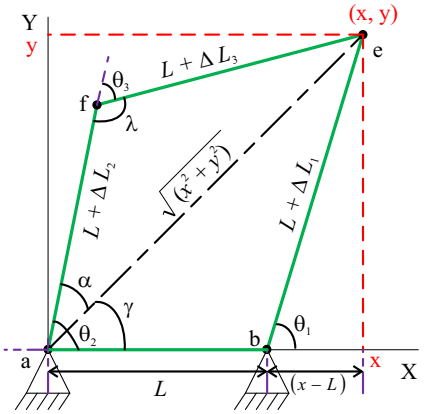

Fig. 7. Inverse-kinematics solution graphical sketch

e) located at position (x, y) required by the SEM with respect to fixed X–Y coordinate system shown. The wider workspace of the new mechanism is depicted in Fig. 6.

3 Inverse kinematics solutions

In order for the EE to reach a pre-specified location described by (x, y) coordinates, the lengths of the piezoelectric actuated links are required to change by $(\Delta L_1,\ \Delta L_2$ and $\Delta L_3)$ from the initial non actuated position. The change in links lengths gives the mechanism an associated unique set of angular positions described by $(\theta_1,\ \theta_2$ and $\theta_3)$ as shown in Fig. 7. The required amount of change in piezoelectric actuated links along with the associated set of angular positions can be bundled in a single inverse kinematics solution vector $\Theta^k = \left[\Delta L_1^k,\ \Delta L_2^k,\ \Delta L_3^k,\ \theta_1^k,\ \theta_2^k,\ \theta_3^k\right]^\top$. The inverse kinematics solution of the four bar mechanism with three-piezoelectric actuated links has been previously obtained using a numerical search technique [24]. The numerical solution acquired represents only one solution among infinite possible solutions for the mechanism. Moreover, it does not represent the optimized solution for the mechanism if it is required to move along a specified path of motion. In order to get the optimized solution, it is essential to determine the least possible difference in the amount of change in $(\Delta L_1,\ \Delta L_2$ and $\Delta L_3)$ required to move the EE from one position to another along its path of motion. Hence, it becomes necessary to get all possible solutions at each single EE (x, y) position prior choosing the optimized solution. The latter fact along with the optimization process represents the major contribution of this work.

Figure 7 shows a general required (x, y) position of the EE, a close look reveals that there exists a unique exact solution for ΔL_1. The solution obtained using (1) is bounded by extreme values of link extension and contraction $\Delta L_{\max}$, $\Delta L_{\min}$ dictated by the physical nature of piezoelectric actuated links. If the calculated value of ΔL_1 does not belong to the interval $[\Delta L_{\min}, \Delta L_{\max}]$ then the required (x, y) position is simply out of reach of the mechanism, therefore the solution is rejected immediately. Equation (2) is used to calculate the value of the associated angular position of link-1 (θ_1) due to the recent change of its length.

$$\Delta L_1 = \sqrt{(x - L)^2 + y^2} - L\,, \tag{1}$$

$$\theta_i = \mathrm{Atan}\,2(y, x - L)\,. \tag{2}$$

Links-2 and 3 on the other hand, can take infinite number of configurations to reach the desired EE point (x, y). In order to get all possible configurations, the inverse kinematics solution is carried out by assuming reasonable values of ΔL_2 and θ_2 that are necessary to get the closed form solution of ΔL_3 and θ_3. The operating range for ΔL_2 and θ_2 are described by

$$\theta_{2i} \in [0, \pi], \quad i = 1, 2, \ldots, m, \tag{3}$$

$$\Delta L_{1j}, \Delta L_{2j}, \Delta L_{3j} \in [-\Delta L_{\min}\,,\ \Delta L_{\max}]$$

$$j = 1, 2, \ldots, p., \tag{4}$$

where, m and p are the number of segments over which θ_2 and ΔL_2 are discretized, respectively.

The assumed value of θ_{2i} is used in (5), (6) to calculate the value of angle α_i shown in Fig. 7. The latter is used in (7) along with assumed value of ΔL_{2j} to calculate the value of ΔL_{3j}. Equation (7) is developed based

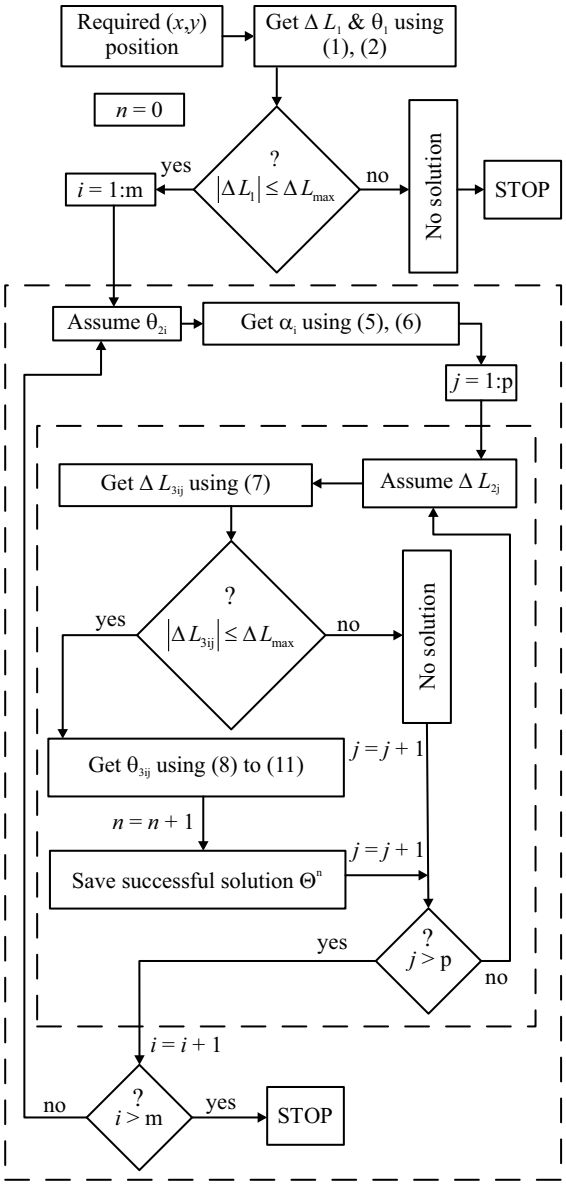

Fig. 8. Schematic diagram of proposed inverse-kinematics solution algorithm

on the cosine law of triangle (acd). Calculated values of $|\Delta L_{3ij}|$ must lie within the range described in (4), otherwise the solution is rejected as it represents an impossible length of piezoelectric actuated link-3. Equations (8) to (10) deploy trigonometric laws over triangle (acd) to calculate λ_{ij} which is used later by (11) to determine the angular position of link-3 (θ_{3ij}). The solution is then repeated using (7) to (11) for all values of ΔL_{2j} with the assumed value of θ_{2i}. Then, another is assumed and the mechanism is solved along all ΔL_{2j} again using (5) to (11) until all values are scanned.

$$\gamma = \operatorname{Atan}2(y, x)\,, \tag{5}$$

$$\theta_{2i} = \alpha_i \pm \gamma \implies \alpha_i = \begin{cases} \theta_{2i} - \gamma\,, & \theta_{2i} \geq \gamma\,, \\ \gamma - \theta_{2i}\,, & \theta_{2i} < \gamma\,, \end{cases} \tag{6}$$

$$\Delta L_{3ij} = -L+ \sqrt{(x^2+y^2)+(L+\Delta L_{2j})^2-2\sqrt{x^2+y^2}(L+\Delta L_{2j})c\alpha_i}, \tag{7}$$

$$c\lambda_{ij} = \frac{(L+\Delta L_{2j})^2 + (L+\Delta L_{3ij})^2 - (x^2+y^2)}{2(L+\Delta L_{2j})(L+\Delta L_{3ij})}, \tag{8}$$

$$s\lambda_{ij} = \frac{\sqrt{x^2+y^2}}{L+\Delta L_{3ij}} \sin\alpha_i\,, \tag{9}$$

$$\lambda_{ij} = \operatorname{Atan}2(s\lambda_{ij}, c\lambda_{ij})\,, \tag{10}$$

$$\theta_{3ij} = \begin{cases} +\big(180 - |\lambda_{ij}|\big), & \theta_{2i} < \gamma\,, \\ -\big(180 - |\lambda_{ij}|\big), & \theta_{2i} > \gamma\,. \end{cases} \tag{11}$$

The inverse kinematics solution described by equations (1) to (11) is illustrated by Fig. 8. For any required EE position (x, y), a total of n successful frames are saved in a general solution matrix Θ of size $(6\times n)$. Where, each column represents a valid inverse kinematics solution and is defined by $\Theta^k = \begin{bmatrix}\Delta L_1^k & \Delta L_{2i}^k & \Delta L_{3ij}^k & \theta_1^k & \theta_{2i}^k & \theta_{3ij}^k\end{bmatrix}^\top$.

4 Optimization

Since there is infinite number of solutions for any position of the EE within the operating workspace, it becomes necessary to optimize those solutions in terms of power required to move the EE from the old position to the new position along the path of motion. The Inverse kinematics solution introduced earlier discretizes the range of the infinite solutions and saves all possible discretized solutions in the general solution matrix . Every column in is a possible solution. If the proposed mechanism is required to fine tune the SEM along a specified path, one can represent the path by a series of required positions that must lie within the working range of the attainable workspace.

Consider the mechanism holding the SEM at an old position defined by $(x_{\text{old}}, y_{\text{old}})$ with the inverse kinematic solution vector $\Theta_{\text{old}} = \begin{bmatrix}\Delta L_{1\text{old}} & \Delta L_{2\text{old}} & \Delta L_{3\text{old}} & \theta_{1\text{old}} & \theta_{2\text{old}} & \theta_{3\text{old}}\end{bmatrix}^\top$. The mechanism is then required to move the EE to another position defined by $(x_{\text{new}}, y_{\text{new}})$. If the proposed inverse kinematics solution algorithm is applied for the new position, then all possible solution vectors are bundled in the solution matrix Θ_{new}. However, one must select one column out of Θ_{new} which represents the minimum power solution $\left(\Theta_{\text{new}}^k\right)_{\min}$. The optimal solution vector must satisfy the least possible difference in change of length of all piezoelectric actuated links. Vector

$$\nabla^k = \Theta_{\text{new}}^k - \Theta_{\text{old}}\,, \quad k = 1, 2, \ldots, n\,, \tag{12}$$

$$\nabla^k = \begin{bmatrix} \Delta L_{1\text{new}} - \Delta L_{1\text{old}} \\ \Delta L_{2\text{new}} - \Delta L_{2\text{old}} \\ \Delta L_{3\text{new}} - \Delta L_{3\text{old}} \\ \theta_{1\text{new}} - \theta_{1\text{old}} \\ \theta_{2\text{new}} - \theta_{2\text{old}} \\ \theta_{3\text{new}} - \theta_{3\text{old}} \end{bmatrix} = \begin{bmatrix} \nabla(\Delta L_1) \\ \nabla(\Delta L_2) \\ \nabla(\Delta L_3) \\ \nabla(\Delta\theta_1) \\ \nabla(\Delta\theta_2) \\ \nabla(\Delta\theta_3) \end{bmatrix} \tag{13}$$

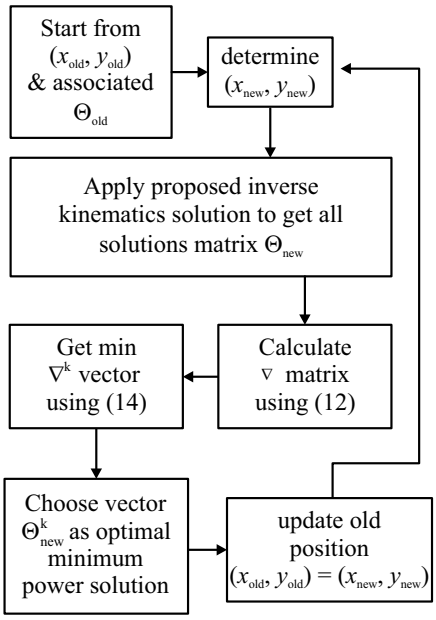

Fig. 9. Minimum power optimization algorithm

defines the amount of change required in each link length and the associated change in the mechanisms angular positions when the EE is required to move from the old position to the new position. The difference matrix ∇ that consists of all ∇^k has an equal size of Θ_{new}.

It is worthy to mention that $\nabla(\Delta L_i$ represents the amount of change required by the piezoelectric actuated link-i when the EE moves from the old to the new position. On the other hand, ΔL_i represents the amount of change required by piezoelectric actuated link-i when the EE moves from the initial unactuated position to any other position in the operating workspace. Moreover, $\nabla(\Delta\theta_i)$ is associated with $\nabla(\Delta L_i)$ and hence depend over their values. Therefore, the optimal solution $(\Theta^k_{\text{new}})_{\min}$ shall be depicted based on the least amount of all $\nabla(\Delta L_i)$ related to a certain EE position. The optimized solution is acquired using

$$(\Theta^k_{\text{new}})_{\min} = \min \sum_{i=1}^{3} \nabla(\Delta L^k_i)\,, \quad k = 1, 2, \ldots, n\,. \quad (14)$$

4.1 Motion along a pre-specified path using the optimized solution

The optimized solution need to be assessed over two types of motion paths. A circular and a linear path of motion that imitates expected shapes of nanowires. The path of motion is discretized into a series of (x, y) positions. The proposed inverse kinematics solution is applied at each single position to obtain all possible solutions. The optimization is then performed over all possible solutions to choose the minimum power single solution that constitutes the least amount of change required by all piezoelectric actuated links to move into the desired position solved for. The motion technique described above is illustrated by Fig. 9.

5 Results

The suggested 3-PZT-FBM was tested by moving the EE along two paths; straight line and circular path. Summation of total gradients for all PZT links L_1, L_2 and L_3 was recorded in Table 1 for the two paths using both optimized and non-optimized solutions. It can be noticed from the table that the sum of gradients of L_1 for any motion is the same in both cases, optimized and non-optimized; this result is expected as the required change in L_1 is governed by the single exact solution described by (1). On the other hand solutions for ΔL_2, ΔL_3 and their associated angular positions, obtained using the proposed inverse kinematic solution, were optimized for each position. Hence, the sum of gradients required in L_2 and L_3 using the optimized solution throughout motion along the circular path is much less than that required by the non-optimized solution for the same path. The latter observation is also true for the straight line path of motion and it shows the value of the proposed minimum power optimization algorithm.

Figures 10 to 12 show the calculated $\nabla(\Delta L_i)$ for the 3PZT-FBM to move from one point to another along the circular path of motion using optimized and non-optimized solutions. It can be noticed from Fig. 10 that both solutions are collinear which emphasizes earlier results shown in Tab. 1. Figure 11 shows how the optimized solution requires less $\nabla(\Delta L_2)$ across the whole path. Figure 12 shows the same result for $\nabla(\Delta L_3)$. For comparison purposes four snapshots of the moving mechanism along

Table 1. Total amount of change in length of all piezoelectric actuated links for optimized and non-optimized solutions for the circular and straight line paths

Sum of absolute changes in μm	Circular Path		Straight line path	
	Non-optimized solution	Optimized solution	Non-optimized solution	Optimized solution
L_1	30.98	30.98	30	30
L_2	5849	1.36×10^{-14}	1960.5	1.36×10^{-14}
L_3	712.68	9.84	211.25	5.23

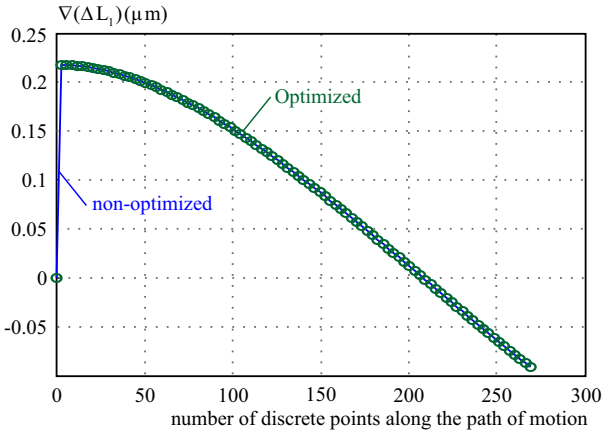

Fig. 10. FourRequired change in Δ_{L_1} along the circular path from point to point

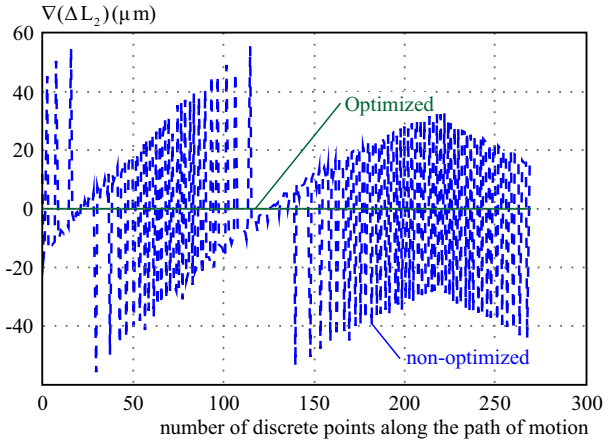

Fig. 11. Required change in Δ_{L_2} along the circular path from point to point

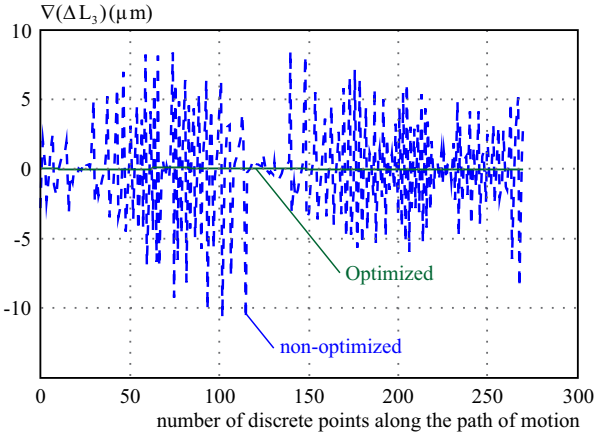

Fig. 12. Required change in Δ_{L_1} along the circular path from point to point

the circular path of motion using both solutions are illustrated in Fig. 13, which shows that $\nabla(\Delta L_i)$ of PZT links are less when the optimized solution is used at all four shown snapshot. Furthermore, the previous results were also obtained for the straight line motion and can be observed in table 1 and Fig. 14 to Fig. 17. Many different paths of motion were tested and similar results were achieved.

6 Conclusions

A four bar mechanism with three piezoelectric links has been proposed as a micro motion tuner for the sample base of an SEM. The suggested mechanism has a wider work space than other lower order PZT four bar mechanisms. An inverse kinematics solution for the suggested mechanism was developed to get a set of all physically possible solutions; this was achieved using an iterative discrete approach based on the minimum physical $\nabla(\Delta L_i)$. The obtained set of solutions for each position was opti-

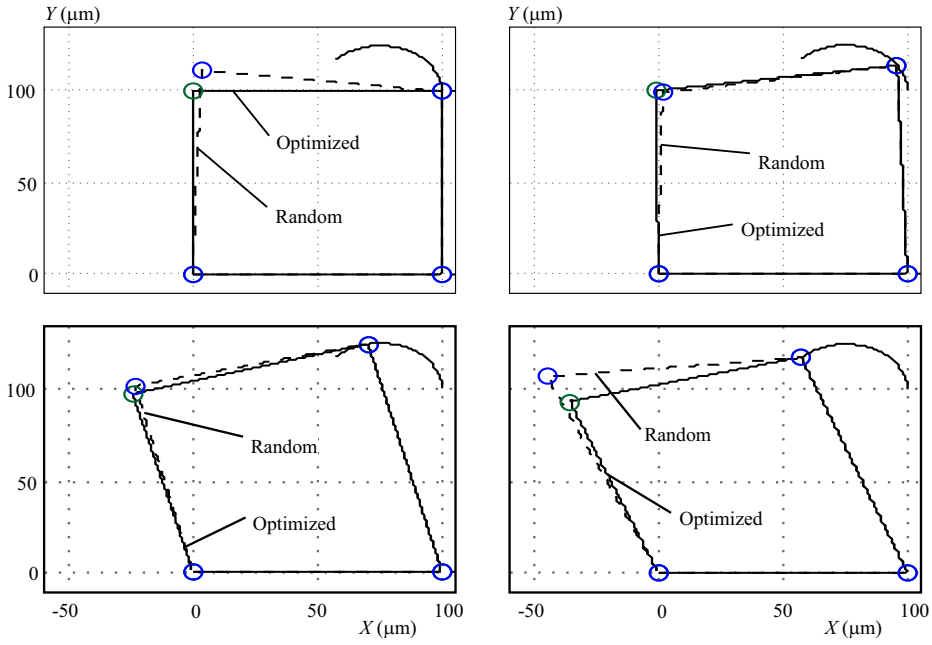

Fig. 13. Optimized *vs* random solution snapshots along the circular path of motion

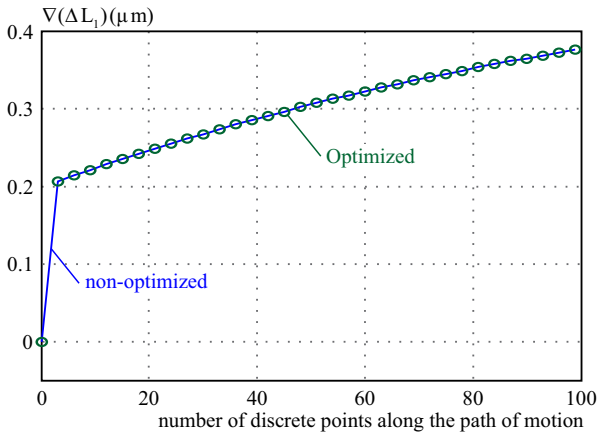

Fig. 14. Required change in Δ_{L_1} along the (SL) path from point to point

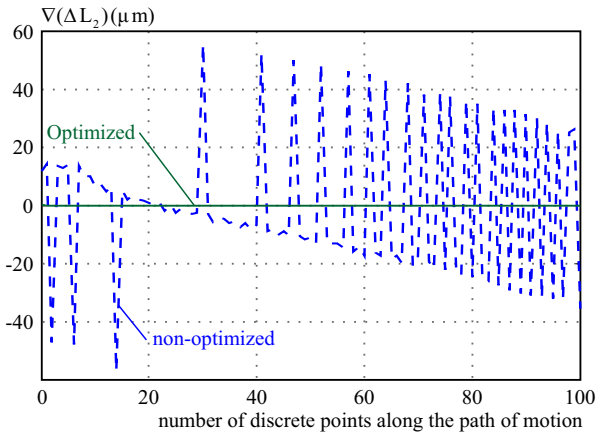

Fig. 15. Required change in Δ_{L_2} along the (SL) path from point to point

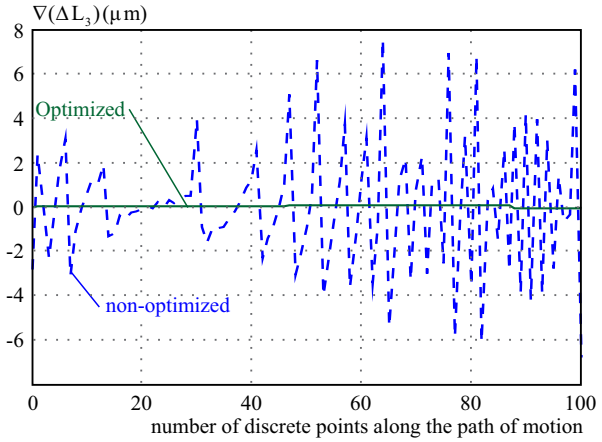

Fig. 16. Required change in Δ_{L_3} along the (SL) path from point to point

mized using the introduced minimum power algorithm shown in Fig. 8. The developed was tested for many paths of motion; two of them were shown in this paper.

Results show the advantage of optimized solution over non optimized solution. The optimized solution required much less power and guaranteed a smooth transition of the mechanism from one point to another along a specified path of motion.

Future work includes developing a GA algorithm to choose the minimum power solution and compare its results with the current work outputs to assess the best among all.

References

[1] B. Deshmukh, S. Pardeshi, R. Mistry, S. Kandharkar, and S. Wagh, "Development of a Four Bar Compliant Mechanism using Pseudo Rigid Body Model (PRBM)", *Procedia Mater. Sci.*, vol. 6, no. Icmpc, pp. 1034–1039, 2014.

[2] G. B. Madhab, C. S. Kumar, and P. K. Mishra, "Modelling and Control of a Bio-Inspired Microgripper", *Int. J. Manuf. Technol. Manag.*, vol. 21, no. 1/2, p. 160, 2010.

[3] K. T. Ooi, "Simulation of a Piezo-Compressor", *Appl. Therm. Eng.*, vol. 24, no. 4, pp. 549–562, Mar 2004.

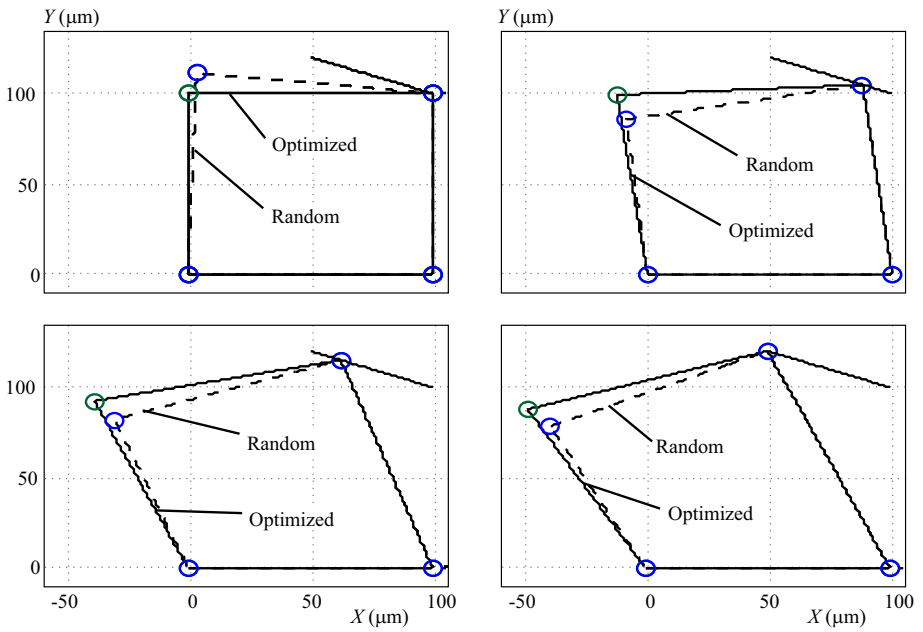

Fig. 17. Optimized *vs* random solution snapshots along the (SL) path of motion

[4] A. Batagiannis, M. Wbbenhorst, and J. Hulliger, "Piezo- and Pyroelectric Microscopy", *Curr. Opin. Solid State Mater. Sci.*, vol. 14, no. 5, pp. 107–115, Oct 2010.

[5] A.-F. Boukari, J.-C. Carmona, G. Moraru, F. Malburet, A. Chaaba, and M. Douimi, "Piezo-Actuators Modeling for Smart Applications", *Mechatronics*, vol. 21, no. 1, pp. 339–349, Feb 2011.

[6] V. Hassani and T. Tjahjowidodo, "Dynamic Modeling of 3-DOF Pyramidal-Shaped Piezo-Driven Mechanism", *Mechanism and Machine Theory*, vol. 70, pp. 225–245, Dec 2013.

[7] H.-Y. Chen and J.-W. Liang, "Control of a 3D Piezo-Actuating Table by Using an Adaptive Sliding-Mode Controller for a Drilling Process", *Comput. Math. with Appl.*, vol. 64, no. 5, pp. 1226–1234, Sep 2012.

[8] Y. Tian, B. Shirinzadeh, and D. Zhang, "A Flexure-Based Mechanism and Control Methodology for Ultra-Precision Turning Operation", /sl Precis. Eng.(, vol. 33, no. 2, pp. 160–166, Apr 2009.

[9] Q. Xu, "Design, Testing and Precision Control of a Novel Long-Stroke Flexure Micropositioning System", *Mechanism and machine Theory*, vol. 70, pp. 209–224, Dec2013.

[10] H. C. Liaw, B. Shirinzadeh, and J. Smith, "Robust Motion Tracking Control of Piezo-Driven Flexure-Based Four-Bar Mechanism for Micro/Nano Manipulation", *Mechatronics*, vol. 18, no. 2, pp. 111–120, Mar 2008.

[11] H. C. Liaw and B. Shirinzadeh, "Enhanced Adaptive Motion Tracking Control of Piezo-Actuated Flexure-Based Four-Bar Mechanisms for Micro/Nano Manipulation", *Sensors Actuators A Phys.*, vol. 147, no. 1, pp. 254–262, Sep 2008.

[12] M.-J. Yang, G.-Y. Gu, and L.-M. Zhu, "High-Bandwidth Tracking Control of Piezo-Actuated Nanopositioning Stages Using Closed-Loop Input Shaper", *Mechatronics*, vol. 24, no. 6, pp. 724–733, Sep 2014.

[13] Y. Qin, B. Shirinzadeh, Y. Tian, and D. Zhang, "Design Issues in a Decoupled XY Stage: Static and Dynamics Modeling, Hysteresis Compensation, and Tracking Control", *Sensors Actuators A Phys.*, vol. 194, pp. 95–105, May 2013.

[14] S. S. Aphale, A. Ferreira, and S. O. R. Moheimani, "A Robust Loop-Shaping Approach to Fast and Accurate Nanopositioning", *Sensors Actuators A Phys.*, vol. 204, pp. 88–96, Dec 2013.

[15] P. V. Chanekar and A. Ghosal, "Optimal Synthesis of Adjustable Planar Four-Bar Crank-Rocker Type Mechanisms for Approximate Multi-path Generation", *Mechanism and Machine Theory*, vol. 69, pp. 263–277, July 2013.

[16] M. Khorshidi, M. Soheilypour, M. Peyro, A. Atai, and M. Shariat Panahi, "Optimal Design of Four-Bar Mechanisms Using a Hybrid Multi-Objective GA with Adaptive Local Search", *Mechanism and Machine Theory*, vol. 46, no. 10, pp. 1453–1465, Oct 2011.

[17] S. Ebrahimi, and P. Payvandy, "Efficient Constrained Synthesis of Path Generating Four-Bar Mechanisms Based on the Heuristic Optimization Algorithms", *Mechanism and Machine Theory*, vol. 85, pp. 189–204, Dec 2015.

[18] M. Sitti, "Piezoelectrically Actuated Four-Bar Mechanism with Two Flexible Links for Micromechanical Flying Insect Thorax", */IEEE/ASME Trans. Mechatronics(, vol. 8, no. 1, pp. 26–36, Mar 2003.*

[19] H. C. Liaw and B. Shirinzadeh, "Robust Generalised Impedance Control of Piezo-Actuated Flexure-Based Four-Bar Mechanisms for Micro/Nano Manipulation", *Sensors Actuators A Phys.* , vol. 148, no. 2, pp. 443–453, Dec 2008.

[20] H. Tang, Y. Li, and J. Huang, "Design and Analysis of a Dual-Mode Driven Parallel XY Micromanipulator for Micro/ Nanomanipulations", *Proc. Inst. Mech. Eng. Part C J. Mech. Eng. Sci.*, vol. 226, no. 12, pp. 3043–3057, Mar 2012.

[21] X. Zhang, J. Lu, and Y. Shen, "Active Noise Control of Flexible Linkage Mechanism with Piezoelectric Actuators", *Comput. Struct.*, vol. 81, no. 20, pp. 2045–2051, Aug 2003.

[22] A. Trevisani, "Feedback Control of Flexible Four-Bar Linkages: a Numerical and Experimental Investigation", *J. Sound Vib.*, vol. 268, no. 5, pp. 947–970, Dec 2003.

[23] M. Y. Al-Azzeh, "Employing Piezoelectric Actuators Manipulating Robots", MSc Thesis, Jordan University of Science & Technology. Dec 2010.

[24] H. K. Khalaf, "Active Control of A Piezoelectric Actuated Four-Bar Mechanism Deployed Robotics Applications", MSc Thesis, Jordan University of Science & Technology. Dec 2012.

Received 15 November 2017

Khaled S. Hatamleh received his BSc (2002) in Mechanical Engineering from JUST, Jordan. Received his MSc (2006) in Industrial Automation Engineering from Yarmouk University, Jordan, and his PhD (2010) in mechanical engineering from New Mexico State University, NM, USA. Currently he is an Assistant Professor at the American University of Sharjah, and JUST. His research areas are: robotics, UAV parameter estimation, IMU, and control systems.

Qais A. Khasawneh received his BSc (1999) From JUST and received his MSc (2002) and PhD (2008) from the University of Akron, USA. He has been serving as an assistant professor in the mechanical engineering department/mechatronics since 2009. His research activities involve MEMS, Nanotechnology, renewable energy, and control.

Adnan Al-Ghasem received his BSc (1996) and first MSc (1999) from Jordan University of Science Technology, Jordan, and his second MSc. (2004) and PhD (2007) in mechanical engineering from Texas A&M University, USA. Currently he is an assistant professor and head of mechanical engineering department at Fahd bin sultan University, KSA, and an assistant Professor in JUST. His research interests are: systems and control, robotics, fluid film bearings, and renewable energy.

Mohammad Abdel Kareem Jaradat received the BSc degree from Jordan University of Science & Technology, Jordan, and the MSc and PhD degrees in mechanical engineering from Texas AM University, College Station, TX, USA. Currently he is an Associate Professor at the American University of Sharjah, and with Jordan University of Science Technology. During his integrated experience several projects, prototypes and publications are conducted, specialized in the following research areas: robotics, artificial intelligent systems, mechatronics system design, sensor fusion, fault diagnostics, intelligent nano-systems, intelligent control, and embedded control systems

Laith Sawaqed (PhD), is the Mechanical Engineering-Acting chairperson of Department. Dr. Sawaqed holds a Bachelor's and Master's Degrees in Mechanical Engineering - Mechatronics from Jordan University of Science and Technology in 2006, 2008, respectively. He received his Doctorate in Mechanical Engineering from University of Maryland - College Park in 2013. His primary area of research has focused on artificial intelligence, robotics, and control systems.

Mohammad Al-Shabi is currently serving as an assistant professor in the Mechanical Engineering Department at University of Sharjah/UAE. He obtained his BSc and MSc in Mechanical Engineering from Jordan University for Science and Technology/Jordan. He obtained his PhD in Mechanical Engineering/Mechatronics from McMaster University/Canada in 2011. His research interest includes Robotics, Control, ANN, Fuzzy, Image Processing, Estimation and Fault Diagnosis.